NeuroImage: Clinical 10 (2016) 96–106

Contents lists available at ScienceDirect

NeuroImage: Clinical

journal homepage: www.elsevier.com/locate/ynicl

Network community structure alterations in adult schizophrenia: identification and localization of alterations

Dov B. Lerman-Sinkoff [a,e,*], Deanna M. Barch [b,c,d]

[a] Department of Biomedical Engineering, Washington University in St. Louis, 1 Brookings Dr., Saint Louis, MO 63130, United States
[b] Neuroscience Program, Washington University in St. Louis, 660 S. Euclid Ave., Saint Louis, MO 63110, United States
[c] Department of Psychological & Brain Sciences, Washington University in St. Louis, 1 Brookings Dr., Saint Louis, MO 63130, United States
[d] Department of Psychiatry & Radiology, Washington University in St. Louis, 660 S. Euclid Ave., Saint Louis, MO 63110, United States
[e] Medical Scientist Training Program, Washington University in St. Louis, 660 S. Euclid Ave., Saint Louis, MO 63110, United States

ARTICLE INFO

Article history:
Received 20 August 2015
Received in revised form 30 October 2015
Accepted 15 November 2015
Available online 18 November 2015

Keywords:
Community structure
Schizophrenia
Resting state functional connectivity
Normalized mutual information
Scrubbing

ABSTRACT

A growing body of literature suggests functional connectivity alterations in schizophrenia. While findings have been mixed, evidence points towards a complex pattern of hyper-connectivity and hypo-connectivity. This altered connectivity can be represented and analyzed using the mathematical frameworks provided by graph and information theory to represent functional connectivity data as graphs comprised of nodes and edges linking the nodes. One analytic technique in this framework is the determination and analysis of network community structure, which is the grouping of nodes into linked communities or modules. This data-driven technique finds a best-fit structure such that nodes in a given community have greater connectivity with nodes in their community than with nodes in other communities. These community structure representations have been found to recapitulate known neural-systems in healthy individuals, have been used to identify novel functional systems, and have identified and localized community structure alterations in a childhood onset schizophrenia cohort. In the present study, we sought to determine whether community structure alterations were present in an adult onset schizophrenia cohort while stringently controlling for sources of imaging artifacts. Group level average graphs in healthy controls and individuals with schizophrenia exhibited visually similar network community structures and high amounts of normalized mutual information (NMI). However, testing of individual subject community structures identified small but significant alterations in community structure with alterations being driven by changes in node community membership in the somatosensory, auditory, default mode, salience, and subcortical networks.

1. Introduction

A growing body of literature suggests that persons with schizophrenia exhibit altered functional brain connectivity (Fornito et al., 2012; Pettersson-Yeo et al., 2011; van den Heuvel and Fornito, 2014), as well as altered anatomical connectivity (Ellison-Wright and Bullmore, 2009; Patel et al., 2011). These findings lend further credence to the "dysconnectivity" theory of this disease (Friston, 1998; Stephan et al., 2006). As such, a better understanding of the patterns of dysconnectivity may yield clinically relevant diagnostic predictors (Sheffield et al., 2015) or improve models of psychosis through explication of subtypes or dimensional models of the disease (Cuthbert and Kozak, 2013) leading to new or improved treatment approaches.

One promising approach to link functional brain connectivity with pathophysiology and etiology is through the use of graph theory and complex network analysis. In these analyses, the data are transformed into a graph by representing locations in the brain as nodes and using measures of connectivity (such as Pearson's correlation) as the connections (also known as ties or edges) between those regions (Bullmore and Sporns, 2009). The graph can then be studied by computing and comparing measures of properties of the graph (see (Rubinov and Sporns, 2010) for an excellent treatment). These approaches have been used to examine brain organization in schizophrenia at the level of the whole brain and within and/or between specific networks and regions. As will be described below, many of these studies point to the suggestion that the organization of brain networks may be altered in schizophrenia. However, few studies have directly tested this hypothesis, which is the goal of the current study.

Several studies of schizophrenia at the whole brain level have suggested that resting state networks in schizophrenia exhibit overall reductions in functional connectivity as compared to healthy controls (Pettersson-Yeo et al., 2011; van den Heuvel and Fornito, 2014).

* Corresponding author at: Campus Box 1125, 1 Brookings Dr., Saint Louis, MO 63130, United States.
E-mail address: lermand@wustl.edu (D.B. Lerman-Sinkoff).

http://dx.doi.org/10.1016/j.nicl.2015.11.011

Graph theoretic analyses at the whole brain level have found significant differences in graph properties between persons with schizophrenia and healthy controls (Fornito et al., 2012; Jiang et al., 2013). For example, multiple studies have found decreased overall local efficiency (Alexander-Bloch et al., 2010; Liu et al., 2008), and decreased clustering and small-worldness in schizophrenia (Alexander-Bloch et al., 2010; Bassett et al., 2012; Liu et al., 2008; Lynall et al., 2010; Ma et al., 2012). While informative, these analyses aggregate across different networks in the brain that themselves may show varying levels of alteration, and thus may mask important psychosis-related differences between networks.

To avoid this issue, a number of studies have examined the properties of specific networks in schizophrenia. Generally, these studies rely on network definitions generated through study of healthy brains (Dosenbach et al., 2007; Fox et al., 2005). While results across such studies are somewhat mixed, a number of studies have found reduced connectivity among regions in the dorsal frontal–parietal network (Cole et al., 2011; Woodward et al., 2011; Zhou et al., 2007) or between dorsal frontal regions and other networks (Cole et al., 2011; Repovs et al., 2011; Zhou et al., 2007). In addition, a number of studies have examined connectivity within the default mode network. While results are again variable, some work suggests increased connectivity within the default mode network (Jafri et al., 2008; Öngür et al., 2010; Whitfield-Gabrieli et al., 2009), as compared to the decreased connectivity found for frontal networks.

Alternatively, rather than studying specific networks, some studies have examined specific types of connections, such as connections with "hub" regions that are thought to be critical for integrating between diverse brain systems (Rubinov and Bullmore, 2013). Two studies (Bassett et al., 2012; Lynall et al., 2010) found evidence for overall decreased probability of hubs or strength of hubs in schizophrenia (Bassett et al., 2012) and localized decreases to temporal association and limbic areas (Rubinov and Bullmore, 2013). Alexander-Bloch and colleagues found that individuals with childhood onset schizophrenia (COS) had similar spatial patterns of hub locations, but that there was significantly increased hub strength in the bilateral dorsolateral prefrontal cortex, right anterior medial cortex, and right inferior parietal lobule (Alexander-Bloch et al., 2012). Thus, a growing body of evidence suggests that there are differential patterns of dysconnectivity across different brain networks in schizophrenia.

Taken together, the results from the whole brain, specific network, and specific connections studies suggest that the underlying community structure (how nodes organize into tightly connected modules or communities) of brain networks in schizophrenia might be fundamentally altered. However, few studies have directly examined community structure alterations. In a series of two studies, Alexander-Bloch and colleagues found evidence in COS demonstrating significant decreases in network modularity (Alexander-Bloch et al., 2010) as well as fundamental differences in community structure (Alexander-Bloch et al., 2012). Their work was the first to demonstrate alterations in community structure of brain functional networks, but used an atypical (COS) population of individuals with schizophrenia. Thus, the present study assesses whether alterations in community structure are unique to COS or are present in a more typical schizophrenia population.

It is important to consider subject head motion when applying network analyses to resting state fMRI data. Recent discoveries by several independent groups have revealed that head motion induces a nonlinear and distance-dependent artifact into resting state data (Power et al., 2012; Satterthwaite et al., 2012; Van Dijk et al., 2012). Increased subject head motion causes an artifactual increase in the measures of correlation between areas that are spatially close and an artifactual decrease in the measures of correlation between areas that are spatially distant (Power et al., 2012). These findings are especially worrisome, as persons with schizophrenia tend to exhibit greater amounts of head motion during scans than controls. Thus, the present study employed a "scrubbing" strategy (Power et al., 2014) in order to reduce the effects of motion upon measures of network community structure.

Here, we present the results of our study of the alterations in brain network organization in adults with stable schizophrenia while stringently controlling for sources of imaging artifacts. We combined two similar but separately collected resting state fMRI datasets in order to maximize our ability to examine community structure alterations in schizophrenia compared to demographically matched healthy controls. Resting state data were pre-processed using "scrubbing" methods to stringently control for sources of imaging artifacts and other artifacts (Power et al., 2014). The resultant correlation matrices were analyzed using graph theory and information theory analyses similar to those in Alexander-Bloch et al. (2012). We examined the question of whether the community structure of resting state brain networks in schizophrenia is altered compared to healthy, demographically matched controls.

2. Materials and methods

2.1. Participants

There were two groups of participants: individuals with schizophrenia (SCZ) and demographically similar healthy controls (CON). The participants were drawn from two separately collected resting state functional magnetic resonance imaging (rs-fMRI) data sets. One data set was reported on in 2011 (Repovs et al., 2011). The other was not previously published. The study inclusion and exclusion criteria were similar across the two data sets: SCZ participants all met DSM-IV diagnostic criteria for schizophrenia, were in outpatient treatment, and were on a stable medication regimen for at least two weeks. CON participants had no lifetime or history of Axis I psychotic or mood disorders and no first-degree family members with psychotic mood disorders. CON and SCZ participants were excluded if they: 1) met DSM-IV diagnostic criteria for substance dependence or severe/moderate abuse during the prior three months; 2) met DSM-IV diagnostic criteria for mental retardation; 3) had a clinically unstable or severe medical disorder; or 4) had current or past head trauma with documented neurological sequelae or loss of consciousness. This resulted in a combined initial 83 SCZ participants and 91 CON participants. Participants were further excluded for several reasons, including: a) 30 CON and 37 SCZ excluded due to motion scrubbing (see below); b) 12 CON and 1 SCZ excluded due to age; c) 7 CON for within-group relatedness (see below); and, d) 1 CON and 1 SCZ due to irrecoverable data corruption during processing. This yielded a final count of n = 41 CON and n = 44 SCZ. Table 1 presents the demographic and clinical characteristics of the retained participants. Participants excluded due to motion were significantly older than the participants that were retained post-scrubbing (Table S1), but did not differ on gender or parental years of education.

In one of the studies described above (Repovs et al., 2011), we recruited healthy controls and their first degree siblings. Prior research has shown that some aspects of functional connectivity are heritable (Glahn et al., 2010). Thus, because only one group contained related individuals, potentially biasing results, only one sibling from a pair of siblings was included in the control group. The sibling with the greatest amount of data remaining after motion scrubbing (described below) was included and data from the second sibling excluded. This resulted in the exclusion of an additional 7 CON participants that had data that would otherwise meet all other inclusion requirements.

2.2. fMRI pre-processing

Both studies were acquired on the same Siemens 3T Tim Trio (Siemens, Erlangen, Germany) scanner at the Washington University in St. Louis Neuroimaging Laboratory facility. Resting state functional magnetic imaging (rs-fMRI) images using blood oxygenation level-dependent (BOLD) contrast were acquired using an asymmetrical spin-echo, echo-planar T2* sequence with (TR = 2200 ms or 2000 ms

Table 1
Demographics, clinical assessments, and motion parameters from participants.

Group	CON (N = 41)		SCZ (N = 44)		Stats
	Mean	SD	Mean	SD	
Age (years)	28.10	8.08	31.59	9.34	$F(1,83) = 0.993$, $p = 0.322$
Gender (% male)	54%		75%		Fishers exact X^2 test $p = .045$
Highest parental years of education	14.54	1.60	13.61	3.59	$F(1,83) = 2.319$, $p = 0.132$
Subject years of education	14.07	1.72	13.11	2.10	$F(1,83) = 5.245$, $p = 0.025$
IQ — WAIS scaled score	10.51	3.10	8.95	3.65	$F(1,83) = 4.470$, $p = 0.037$
SAPS positive symptoms	0.049	0.22	3.43	2.82	$F(1,83) = 58.49$, $p < 0.000$
SAPS disorganized symptoms	1.37	1.34	3.11	2.62	$F(1,83) = 14.705$, $p < 0.000$
SANS negative symptoms	1.07	1.77	8.34	3.28	$F(1,83) = 158.06$, $p < 0.000$
Olanzapine equivalents	–	–	19.86	18.82	
Mean frames lost in subjects retained after scrubbing	93.63	66.62	105.66	105.66	$F(1,83) = 0.993$, $p = 0.322$
Mean frames remaining after scrubbing	254.9	62.5	244.2	53.6	$F(1,83) = 0.723$, $p = 0.397$
Mean pre-scrubbing FD (framewise displacement) in mm	0.16	0.13	0.16	0.10	$F(1,83) = 0.161$, $p = 0.689$

depending on study, TE = 27 ms, FoV = 256 mm, 90° flip angle, $4 \times 4 \times 4$ mm^3 voxels). Participants were presented with a fixation crosshair and data were collected in two eyes-open runs of 164 or 180 frames each, depending on study. Each resting-state scan was pre-processed by correcting slice-timing, realigning to compensate for rigid body movement, normalizing to a whole-brain mode intensity of 1000, linearly transforming to Talairach atlas space, and resampling to 333 space. Pre-processing was completed using a set of in-house tools written by Avi Snyder in the Washington University in St. Louis Neuroimaging Labs.

Anatomical T1 images were collected using a magnetization prepared rapid gradient echo (MPRAGE) sequence with either $1.2 \times 1 \times 1$ mm or $1 \times 1 \times 1$ mm voxels, depending on study. These images were segmented using Freesurfer-5.3 on the Washington University Center for High Performance Computing supercomputer. These segmentations were then resampled to 333 space and used to generate subject-specific nuisance regressor seed masks for white matter, ventricular, and global signals.

Participants' rs-fMRI scan runs were then pre-processed according to the methodology presented in Power et al. (2014) using a suite of MATLAB (The Mathworks, Natick, MA) tools developed by Jonathan Power in the Petersen and Schlaggar labs at Washington University in St. Louis. The first five frames of each scanning run were removed to allow BOLD signal dynamics to reach steady state. Each run was then: (1) demeaned and detrended to compensate for scanner offset and drift; (2) nuisance signals were regressed out using the Freesurfer generated seed masks and rigid-body motion estimates generated by a 24 parameter Volterra expansion (Friston et al., 1996; (3) frequency filtered using a zero phase, second order Butterworth filter with passband $0.009 \text{ Hz} < f < 0.08$; and (4) spatially blurred using a 6 mm FWHM Gaussian filter.

Motion-derived artifact was "scrubbed" by generating temporal masks censoring frames exceeding a framewise displacement (FD) of greater than 0.2 mm. Frames were additionally censored if there were not 5 contiguous frames. That is, if scrubbing censored frames resulted in a set of 1–4 non-censored frames that were discontinuous from other frames, then those 1–4 frames were additionally censored. Entire runs were censored if there were not at least 50 frames per run, and a participant had to have at least 100 usable frames to be included in the analyses. The entire dataset was then reprocessed using the steps described above excluding the censored frames and interpolating between epochs of low (uncensored) motion and high (censored) motion in order to prevent spread of motion-related artifact into adjacent non-censored frames. This resulted in the exclusion of 30 CON and 37 SCZ participants leaving a final N = 41 CON and N = 44 SCZ participants with analyzable data. Two less stringent FD criteria (0.5 mm and 1.0 mm) were also examined and assessed for effects upon downstream analyses of community structure (described below) (Figs. S4, S5 and Tables S4, S5). The less stringent FD criteria yielded higher NMI values in general and somewhat diminished significance of the strongest results of the Phi-test (see below). It is possible that this might reflect motion-induced structured artifact, or alternatively, increased structured signal content in the data. Overall, the findings with the less stringent FD criteria did not substantively alter our conclusions and thus in the manuscript we focus on the most conservative approach (FD = 0.2 mm).

2.3. Region of interest selection

Regions of interest (ROIs) were selected by generating masks corresponding to spheres with 10 mm diameters centered at the set of 264 Talairach coordinates described in Power et al. (2011). These regions were generated by combing two approaches: 1) a set of 151 stably activating and non-overlapping regions were identified from a meta-analysis of task fMRI studies, and 2) a set of 193 non-overlapping ROIs generated using a resting state functional connectivity mapping approach in forty young, healthy adults. When analyzed using a network analysis approach, these regions were found to organize and recapitulate many known neural systems and thus represent a reasonable and validated choice for exploring the changes in neural functional connectivity in schizophrenia. For each subject, timecourses corresponding to each of the 264 ROIs were extracted and cross-correlated to generate a 264×264 matrix of Pearson's ρ correlation coefficients. This matrix represents the correlation between any two ROIs from a given subject's rs-fMRI data. The effect of excluding ties between nodes within close proximity (20 mm) was also examined due to concern in the literature (Power et al., 2011) for these ties to be more affected by motion artifact and non-biological noise (Fig. S3, Table S3). While this resulted in some modest alterations in node significance in the Phi-test (described below) and a decrease in shared structure (e.g., overall reduced similarity in community structure), the overall results were similar and did not alter our conclusions. As such, we present the results with the close proximity ties included.

2.4. Group-level analyses of community structure

While development of algorithms to determine community structure is an active area of research (Fortunato, 2010), several methods, such as Newman's spectral modularity (Newman, 2006) and Infomap (Rosvall and Bergstrom, 2008), have emerged and have been used in the neural imaging literature to develop maps of normative human brain organization (Blumensath et al., 2013; Power et al., 2011; Rubinov and Sporns, 2010). We chose to use Infomap because it has been successfully used to characterize the functional organization of the healthy human brain (Power et al., 2011) as well as its high performance in detecting communities in graphs (Fortunato, 2010; Rosvall and Bergstrom, 2008).

To examine group level community structure, 264 × 264 group-level mean correlation matrices were generated by taking the mean edge correlation coefficient (the correlation between two ROIs) of participants' Fisher R-to-Z transformed data for each group. This group average correlation matrix was then sparsified and binarized at a range of thresholds and then processed with Infomap to generate a partitioning of the graph into communities. Sparsification was accomplished by taking the 264 × 264 group mean correlation coefficient matrix and removing the weakest correlation coefficients until the density of remaining correlations (also known as tie-density) reached a specific value. Sparsification in this manner allows for comparison between different graphs that may have different mean levels of correlation and was performed such that each group had ten graph representations of their data at the strongest 10% to 1% correlation values in 1%-density steps. The matrices were then binarized for each tie-density level by setting all remaining correlations to a value of one. Community structure was then determined for each group's ten sparsified graphs using the Infomap algorithm (Rosvall and Bergstrom, 2008). This resulted in a 10 × 264 (tie-density × ROI) matrix for each group comprised of integer values representing community assignments at each element. Communities that were comprised of less than five unique ROIs at a given tie-density were censored from further analysis due to the lack of plausible biological explanations for such communities. Weighted sparsified graphs were also examined and results can be found in the supplement (Table S6 and Fig. S6). These analyses resulted in some modest alterations in node significance in the Phi-test (described below) and a decrease in shared structure (e.g., overall reduced similarity in community structure). However the overall results were similar and did not alter our conclusions.

Group-level community structure was visualized by assigning a color to each community's set of ROIs. This was then graphed in two ways: (1) as a two dimensional graph with the x axis representing decreasing tie density percentages and the y axis representing the ROI as numbered in the Power, 2011 atlas; and (2) by overlaying 10 mm diameter spheres colored by community and placed at the appropriate coordinates on the PALS-B12 atlas using Caret 5.65 (Van Essen, 2005; Van Essen and Dierker, 2007; Van Essen et al., 2001). Nodes that were within 5 mm of midline were reflected to the contralateral hemisphere to account for errors in MRI alignment and registration.

Because the integer value and color representing a community assignment is stochastically assigned by Infomap, visual comparison across groups was simplified by recoloring matching networks across groups. The CON group was chosen as a template and the color of ROIs of matching communities in SCZ were recolored to match CON, without changing community assignments. For example, if ROIs the in the visual network were colored green in CON, then the ROIs in the visual network in SCZ were also colored green, even if the ROIs were not identical across groups.

In order to quantitatively determine the extent to which group-level network structures were similar across groups, normalized mutual information metrics (described below) were computed between the CON and SCZ groups in the current study, as well as between the CON and SCZ groups in the current study and the two cohorts of normative participants described in Power et al. (2011). This pairwise similarity measure, normalized mutual information (NMI), varies between zero (complete dissimilarity) and one (identical community assignments). MATLAB tools provided by Jonathan Power (available at http://www.nitrc.org/projects/graphtools/) were used to compute NMI using information theory definitions (see Eqs. (16.2)–(16.6) for reference, (Manning et al., 2008)). X and Y are individual graphs with $X = \{x_1, x_2, \ldots, x_n\}$, and $Y = \{y_1, y_2, \ldots, y_n\}$ representing community assignments of node x_n and y_n; I(X, Y) is the mutual information between X and Y; and, H(X) and H(Y) are the entropy of X and Y. These computations were performed per tie-density and resulted in a NMI value of similarity between community assignments for each tie-density.

$$I(X,Y) = \sum_{k}^{n}\sum_{j}^{n} P\left(x_k \cap y_j\right) * \log\frac{P\left(x_k \cap y_j\right)}{P(x_k) * P\left(y_j\right)}$$

$$H(X) = -\sum_k P(x_k) * \log(P(x_k)) \quad NMI(X,Y) = \frac{I(X,Y)}{(H(X) + H(Y)/2}$$

2.5. Subject-level analyses of community structure

The above methods are useful for qualitatively describing the group level differences between CON and SCZ. However, they do not allow statistical evaluation of the degree of variability among individuals within a group nor do they allow for determination of whether the community structure differs significantly between groups. To do so, graphs were generated and community detection performed as described above except that graphs were generated for each individual subject at each tie-density rather than group average graphs at each tie-density. As above, communities with less than five nodes were censored from downstream analyses.

The normalized mutual information (NMI) pairwise similarity metric can be extended to test for group differences. If some variance in the community structure data is reliably explained by group membership greater than chance, then the mean NMI between all possible pairs of participants within that group should be higher than the mean NMI of pairs of participants chosen from random groups. As the underlying distribution of group mean NMI is unknown, statistical tests upon the mean NMI require generation of a null-distribution through a permutation method. The method developed by Alexander-Bloch et al. (2012) was modified to run in MATLAB. This method used group label permutation to determine when participants within a diagnostic group were more similar than participants across diagnostic group. An NMI value was calculated for each pair of participants at all tie-densities and used to calculate the true mean within-group NMI as well as the true mean NMI for all between-group pairs. Group labels were then randomly shuffled 10,000 times and the permuted mean "within-group" NMI was calculated at each tie-density. p-Values were then calculated separately for each tie-density as the count of the number of instances when the permuted mean within-group NMI was greater than the true mean within-group NMI, divided by the number of permutations.

2.6. Phi-test and heat maps of community structure

The NMI permutation test described above indicates whether group membership makes a significant difference for community structure. However, it does not reveal how community structures may differ across groups or how the community assignment of specific ROIs may differ across groups. To identify the ROIs responsible for group differences in NMI, we used a second permutation test developed by Alexander-Bloch et al. (2012). This tested whether an ROI's participation in a given community varied between participants more when they belonged to different diagnostic groups than when they belonged to the same diagnostic group. For each subject and tie-density, a 264 × 264 binary-valued matrix was generated corresponding to whether, for a given ROI, all other ROIs shared the same community. ROIs were marked as either participating (1) or not participating (0) in the given ROI's community. For example, Fig. 1 shows three 9-ROI toy graphs generated on the same ROIs and their corresponding binary community assignment matrices. The binary community assignment matrices were then used to generate subject-by-subject node similarity measures using Pearson's Phi (similar to Pearson's correlation coefficient, but for binary values). The community membership column

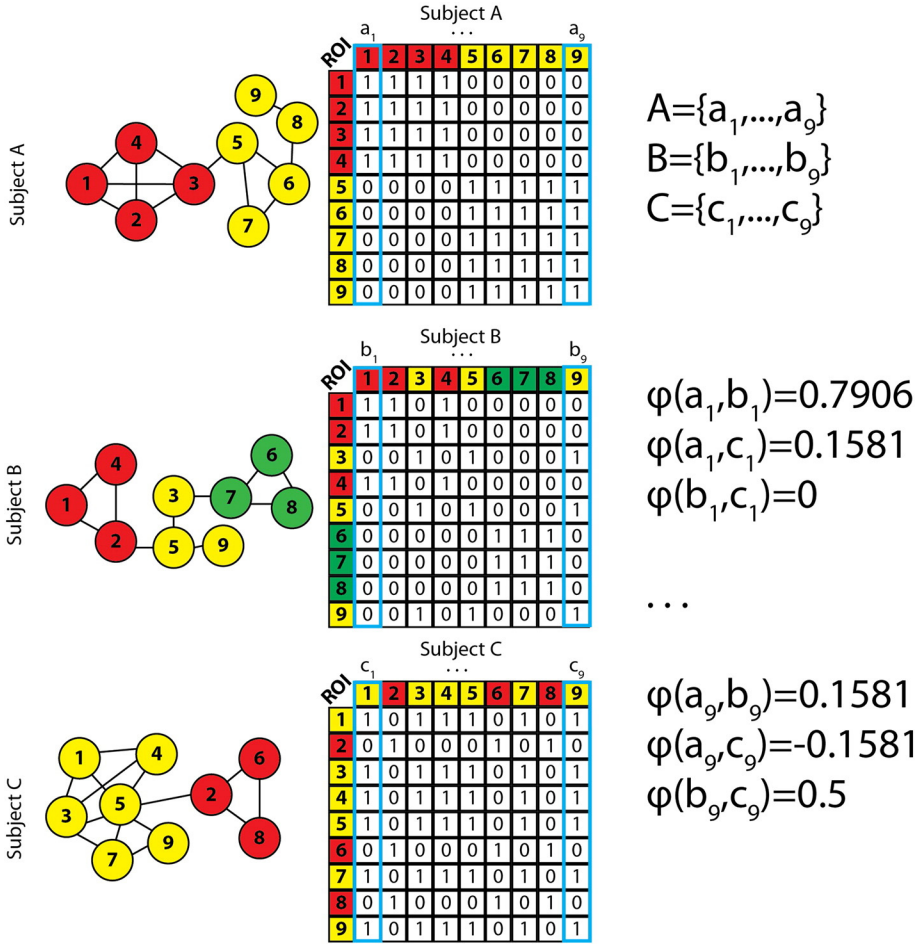

Fig. 1. Example schematic of generation of ROI and subject pair Phi values. Left column: illustration of three toy graphs comprised of the same set of ROIs but with different community structures. Middle column: the binary matrix corresponding to which ROIs belonged to the same community. Right column: each subject's data (capital letter) are comprised of the set of column vectors from the subject's binary matrix of community membership. The value of Pearson's Phi is computed for all subjects' nodes across the corresponding columns (e.g.: a1 with b1, but not a1 with a2).

for each subject's ROI 1 was correlated to each other subject's ROI 1 column using Pearson's Phi, and so forth for all other ROIs. As with NMI, the pair-wise similarity metric was extended to test for group differences through permutation of group labels. The true within-group mean Phi was calculated for all within-group subject-by-subject ROI pairs, then labels were shuffled 10,000 times, and mean permuted within-group Phi values were calculated and compared with the real data to generate a p-value. Values returned from this procedure were similar to NMI in that they are both pairwise similarity metrics, but Phi provides per-ROI resolution. Thus, for each tie-density, a set of 264 p-values was generated corresponding to whether a given ROI's community was more similar for participants from the same group than permuted groups. The set of 264 p-values generated at each tie-density were corrected for multiple comparisons using FDR (Benjamini and Hochberg, 1995) with MATLAB tools available at (http://www.mathworks.com/matlabcentral/fileexchange/27418).

2.7. Seed map verification of Phi-test results

The Phi-test identified nodes whose community assignment significantly varied across the two groups. To validate these results, traditional seed map analyses were performed using ROIs that were identified as significant across two or more tie density thresholds. In-house software (FIDL 2.65, http://www.nil.wustl.edu/labs/fidl/index.html) was used to perform group t-tests for differences in connectivity for "CON–SCZ" using an unequal assumption of variance and a Monte-Carlo correction factor for significance requiring a cluster of 35 or more voxels with a Z-score greater than or equal to 2.5. Test results were visualized using Connectome Workbench software (http://www.humanconnectome.org/software/connectome-workbench.html) at a threshold of $Z > 2.5$ and $Z < -2.5$.

3. Results

3.1. Demographics

Following scrubbing and exclusions (detailed in Table 1), N = 41 CON and N = 44 SCZ participants retained sufficient data for analysis. The retained participants did not differ on the number of retained or lost frames, pre-scrubbing mean framewise displacement, age, or parental years of education. Participants did significantly differ on gender (more males in SCZ), personal years of educational attainment (less in SCZ), IQ (less in SCZ), and clinical symptoms (more in SCZ).

3.2. Group level analyses

Qualitative examination of group average network structure (Fig. 2) as well as the full unthresholded correlation matrices (Fig. S2) revealed that overall, resting state connectivity and network structure was relatively well preserved in SCZ. This visual similarity was quantified using normalized mutual information (NMI) between the mean CON and SCZ network structures (Table 2). This revealed a high level of shared information confirming the overall visual similarity of network structures

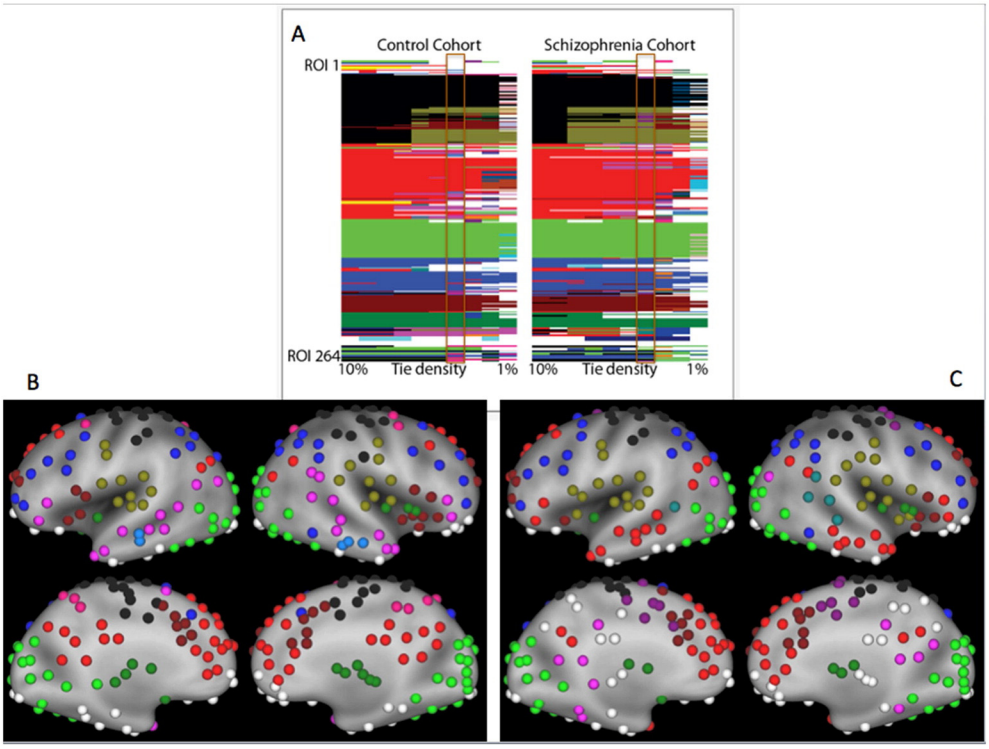

Fig. 2. Group level community structure revealed overall similar structure between CON and SCZ cohorts. Panel A: ROI numbers corresponding to the Power 264 atlas are on the vertical axis and tie densities are on the horizontal axis. Regions are colored by community assignment and white regions correspond to communities with less than five ROIs. Panel B: CON ROIs colored by communities detected at the 4% tie density and superimposed on the very inflated PALS-B12 atlas. Panel C: SCZ ROIs colored by communities detected at the 4% tie density and superimposed on the very inflated PALS-B12 atlas.

(across tie density mean NMI = 0.74, std = 0.03). Additionally, NMI between our CON and SCZ groups was computed with the two cohorts of healthy controls described in Power et al. (2011) revealing a high level of agreement between our participants and the healthy participants described in Power et al. (2011). The average NMI between our CON and SCZ groups (0.74) was as high as the average NMI between our CON group and the two CON groups from Power et al. (2011) (0.73). Thus, the overall network structure differences between our controls and schizophrenia participants were on the same order as differences between our community control participants and the healthy Washington University community population used in the Power 2011 study.

3.3. Subject level analyses

Subject level community detection generated ten sets of network structures for each subject, one at each tie density. Although the group level community structure analyses suggested very similar patterns, the NMI permutation on these individual subject network structures revealed that the mean of all within-group subject pairings was significantly higher than the mean of all between-group subject pairings for all but one tie-density (Table 3). Thus, the community structure was significantly less similar in the permuted groups than within the real groups. Additionally, at all tie densities, the mean within-CON NMI was greater than the mean within-SCZ NMI, implying possibly greater heterogeneity (i.e., less overall shared information) of network structure in the SCZ group.

While NMI permutation is able to assess whether there are significant differences in community structure, it does not indicate the regions responsible for the differences. Follow-up permutation tests of community assignments (Fig. 3), described by Alexander-Bloch et al. (2012), were used to reveal ROIs whose community assignments varied significantly between groups and across most tie densities. Two images were

Table 2
NMI values between CON, SCZ, and the Power 2011 healthy cohorts exhibited high level of similarity of network structure across all three cohorts.

Tie density	CON × SCZ	JP_MAIN × CON	JP_REP × CON	JP_MAIN × SCZ	JP_REP × SCZ
10%	0.79	0.81	0.81	0.75	0.75
9%	0.78	0.79	0.82	0.72	0.74
8%	0.72	0.78	0.82	0.70	0.70
7%	0.73	0.72	0.75	0.70	0.76
6%	0.74	0.68	0.69	0.67	0.69
5%	0.70	0.69	0.70	0.72	0.70
4%	0.72	0.69	0.68	0.73	0.71
3%	0.74	0.70	0.67	0.72	0.68
2%	0.71	0.67	0.66	0.70	0.68
1%	0.77	–	–	–	–
Mean across tie density	*0.74*	*0.73*	*0.73*	*0.71*	*0.71*
Standard deviation	*0.03*	*0.05*	*0.07*	*0.02*	*0.03*

JP_MAIN is the main cohort used in Power et al. (2011); JP_REP is the replication cohort used in Power et al. (2011).

Table 3
NMI permutation testing revealed significant differences between CON and SCZ network structures.

Tie density	p-value: real > permuted data	Mean of all within-group NMI pairings	Mean of all between-group NMI pairings	Mean within-CON NMI	Mean within-SCZ NMI
10%	0.0009	0.256	0.251	0.271	0.243
9%	0.0006	0.273	0.268	0.280	0.267
8%	0.0075	0.291	0.287	0.301	0.281
7%	0.0044	0.314	0.310	0.330	0.300
6%	0.0062	0.331	0.328	0.344	0.319
5%	0.0194	0.356	0.353	0.371	0.343
4%	0.0306	0.370	0.368	0.386	0.357
3%	0.0171	0.380	0.378	0.399	0.364
2%	0.1574	0.373	0.372	0.395	0.354
1%	0.0143	0.315	0.312	0.339	0.294

generated to visualize the pattern of significance across ROIs and across tie-densities. First, nodes were first grouped into their (Power et al., 2011) networks using FDR corrected $p < 0.05$ as the significance criterion, and the percent of significant nodes within a network were counted. As shown in Fig. 3, there was variability across groups in the community assignments of a relatively high percentage of ROIs in the subcortical network across all tie density levels. In addition, there was variability across groups in the somatosensory hand and mouth, auditory, default mode, and salience networks for a small percentage of nodes. To further illustrate the pattern of significant ROIs, an aggregate "heatmap" of significance was generated by summing the number of tie-densities for which a given ROI was significant at an FDR corrected $p < 0.05$. These ROIs, colored by the count of significant tie-densities, were overlaid on the PALS-B12 atlas using Caret and each ROI was surrounded with a colored circle corresponding to its a priori network from the Power atlas (Power et al., 2011). This map (Fig. 4) illustrates the spatial location and relative consistency across tie densities of ROIs contributing to differences in NMI and community structure differences between CON and SCZ. This map revealed ROIs showing significant group effects at multiple tie densities in bilateral thalamus, as well as significant effects in the bilateral paracentral lobules, left anterior cingulate, and the right insula and pulvinar (see Table S6 for full details).

To validate the results of the Phi-test, nodes that were found to be significant sources of variation in community participation at two or more tie-densities were identified and used to perform seed map analyses. These ROIs included the left (Fig. 5) and right (Fig. S7) medial dorsal nuclei, the left paracentral lobule (Fig. 6), as well as several others (see Table S7 and Figs. S8–S11). Examination of the ROI in the left medial dorsal thalamic nucleus revealed clear differences in connectivity between CON and SCZ (Fig. 5) with SCZ exhibiting bilaterally symmetric hyper-connectivity with somatomotor and somatosensory regions and hypo-connectivity with prefrontal, striatal, and cerebellar regions. The corresponding ROI in the right medial dorsal nucleus exhibited similar results (Fig. S7). Examination of the left paracentral lobule/BA 31 exhibited significant dysconnectivity (Fig. 6), with SCZ exhibiting cerebellar dysconnectivity, hypo-connectivity with somatomotor, right insular, and left posterior cingulate, as well as hyper-connectivity with the inferior parietal lobule and frontal gyri.

4. Discussion

The goal of the current study was to determine whether the community structure of resting state functional connectivity networks was altered in adults with schizophrenia. Our results suggested that while network structures were overall quite similar, especially at the group level, there are small but significant changes in functional network community structure in persons with schizophrenia. Specifically, group average network structures exhibited highly visually similar community structure across tie densities between the two groups. Quantitative follow-up examining NMI between group average network structures confirmed the visual similarities at matched tie densities. However, statistical evaluation across individual participants revealed evidence for small but significant differences in network community structure. Follow-up analyses revealed that alterations in node community participation in the subcortical, somatosensory, auditory, default mode, and salience networks were the strongest contributors to differences in network community structure. Finally, the nodes that were most strongly responsible for alterations in community participation exhibited statistically significant patterns of dysconnectivity in a seed map analysis.

As described above, the group-level analyses suggested that the network community structure was relatively intact in adults with

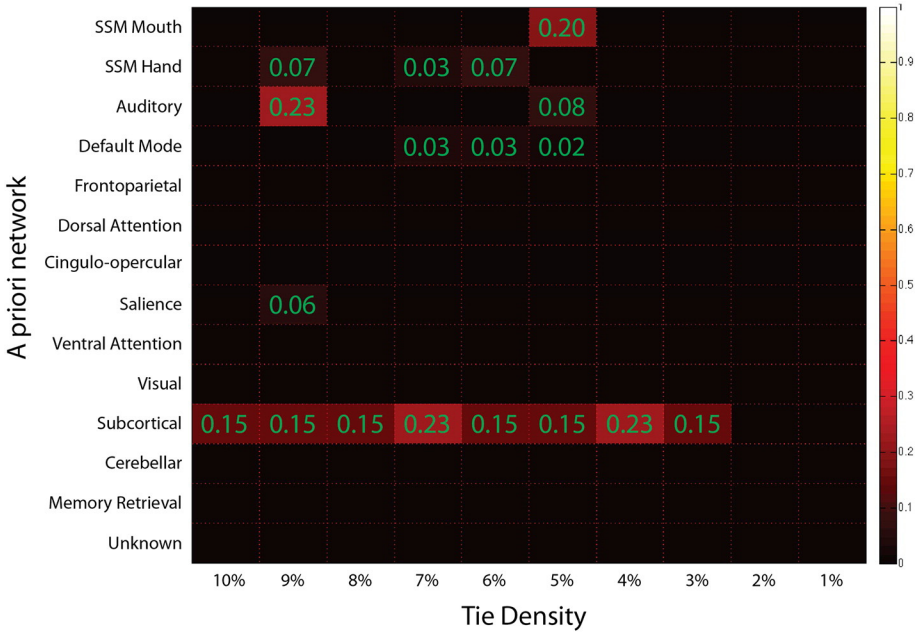

Fig. 3. Phi test results exhibited alterations in node community membership in the subcortical, salience, auditory, somatomotor, and default mode networks. Each network is colored by the fraction of nodes with significant (FDR corrected $p < 0.05$) alterations at that tie density.

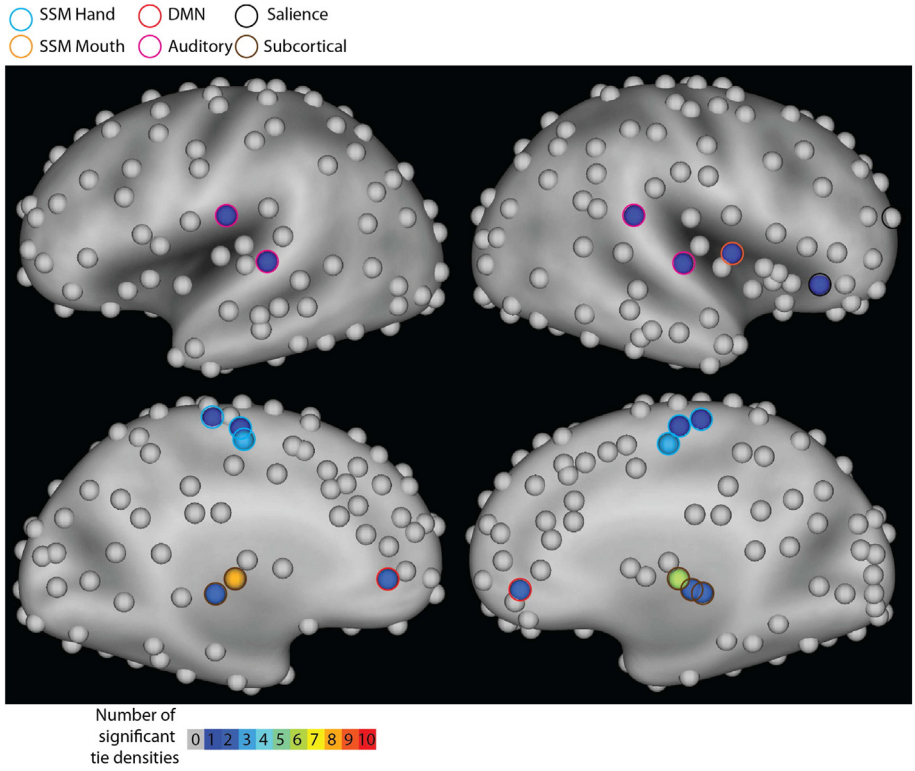

Fig. 4. Phi test heatmap at FDR corrected $p < .05$ revealed significant community assignment alterations in ROIs including the somatosensory, insular, anterior cingulate, and thalamic regions. ROIs are colored by number of significant (FDR corrected $p < 0.05$) tie densities. Significant ROIs are surrounded by a colored ring corresponding to their a-priori network definitions from the Power et al. (2011) atlas.

schizophrenia. Further, at the group level, both controls and individuals with schizophrenia had near-equal amounts of shared information with both sets of network structures generated using data from two different samples of healthy Washington University students previously reported in Power et al. (2011). Thus, at the group level, the amount of variation between the present community controls and participants with

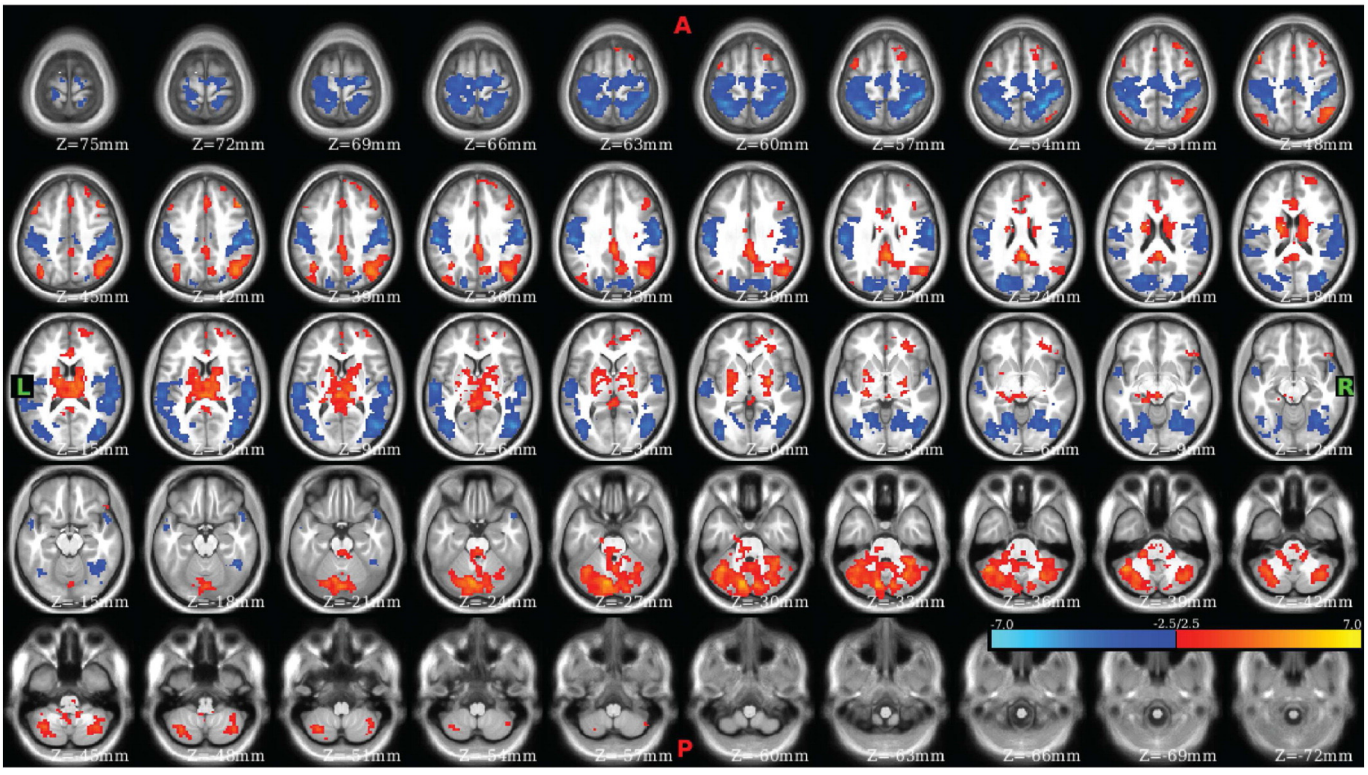

Fig. 5. Left medial dorsal nucleus exhibited significant dysconnectivity in schizophrenia. Contrast CON–SCZ. Red voxels correspond to statistically significant CON > SCZ connectivity and blue voxels correspond to statistically significant SCZ > CON connectivity.

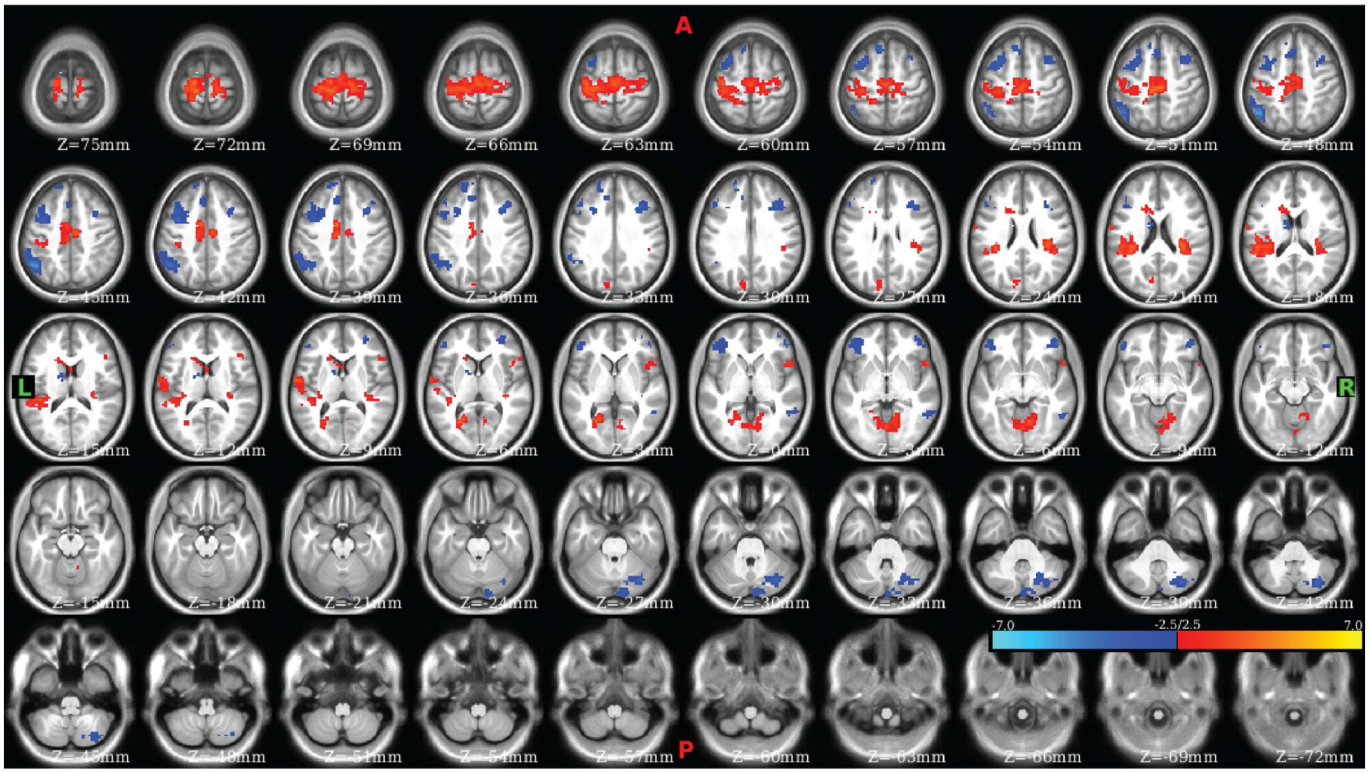

Fig. 6. Left paracentral lobule/BA 31 exhibited significant dysconnectivity in schizophrenia. Contrast CON–SCZ. Red voxels correspond to statistically significant CON > SCZ connectivity and blue voxels correspond to statistically significant SCZ > CON connectivity.

schizophrenia was similar to the amount of variation between the present controls and the controls used in the Power et al. (2011) study. As such, although there are some significant differences in community structure apparent upon finer grained analysis, these results suggest that at least at a gross level, there is relatively well-preserved functional structure of organization of the human brain in schizophrenia, though further work will be required to replicate this finding.

Although community structure appeared relatively well preserved at the group level, examination of subject level network structures and statistical assessment via permutation testing did identify significant differences in community structure between participants with schizophrenia and healthy controls. Follow-up testing revealed that community participation of nodes in the somatosensory hand and mouth, subcortical, auditory, default mode, and salience networks were the largest contributors to these differences in community structure, though it was still a relatively small percentage of ROIs in each of these networks that displayed group differences in community participation. More specifically, nodes that displayed group differences were in bilateral medial frontal gyrus and bilateral thalamus, with a minority of additional responsible nodes including the right insula and other locations (Table S6).

These findings are partially consistent with the findings from Alexander-Bloch et al. (2012), which identified primarily right lateral somatomotor and right anterior insular nodes as the those responsible for driving differences in community structure. The present study also identified those nodes as significant, with the additional identification of significant alterations in the contralateral (left hemisphere) somatomotor nodes, as well as significant alterations in bilateral thalamic and mediofrontal nodes. The finding of similarly implicated areas further adds to the evidence that suggests that childhood onset schizophrenia exists on a continuum with adult schizophrenia and shares etiologic factors, but is characterized by a more severe and homogenous presentation (Driver et al., 2013; Rapoport and Gogtay, 2011). However, in our adult sample, the presence of the additional bilateral thalamic and mediofrontal ROIs as well as less consistently significant results in the right insula (compared to Alexander-Bloch and colleagues) implies additional and/or different factors at play in the disease processes between adult onset schizophrenia and childhood onset schizophrenia.

The regions identified by Alexander-Bloch et al. (2012) and the present study have been identified as showing altered connectivity in other studies in schizophrenia as well. For example, Palaniyappan et al. (2013) identified abnormalities in right anterior insular connectivity between the dorsolateral prefrontal cortex and visual cortices using Granger causal modeling performed on resting state fMRI. Moran et al. (2013) also used resting state fMRI and found decreased functional connectivity between the right ventral anterior insula and regions in the default mode network. They also identified decreased group Granger path coefficients in schizophrenia from the dorsal anterior insula to the DLPFC, posterior cingulate cortex, and lateral parietal cortex. Finally, Moran et al. also identified significant decreases in connectivity from the dorsal anterior insula to the DLPFC, and mPFC using structural connectivity modeling. Previous studies have also identified alterations in thalamic connectivity. Specifically, Woodward et al. (2012) identified decreased resting state functional connectivity in schizophrenia between the medial dorsal and right anterior thalamic nuclei and prefrontal regions as well as increased connectivity in schizophrenia between somatosensory and motor areas and the pulvinar and ventrolateral thalamic nuclei. Anticevic et al. (2014a) also identified alterations in thalamic resting state functional connectivity in schizophrenia and found that participants with schizophrenia had increased thalamic coupling to sensory cortices and decreased coupling to prefrontal cortex, striatum, and cerebellum. Anticevic et al. (2014b) and Woodward and Heckers (in press) also identified significant thalamocortical dysconnectivity in schizophrenia, an effect that was independently identified here via the Phi-test and replicated in the seed map analyses. Thus, the present study adds to this body of evidence by demonstrating that not only are there alterations in connectivity strength and directionality in areas such as the insula and

the thalamus, but that these areas may also be contributing to differences in network community structure observed in persons with schizophrenia.

5. Limitations and future directions

First, participants with schizophrenia were on a stable medication regimen at the time of scanning and it is possible that medications influence the patterns of functional connectivity. Second, we did not control for structural brain differences in SCZ beyond standard image registration to an atlas space. Further, there were demographic differences between the groups such that SCZ had lower measures of IQ and decreased years of education, though the groups were not different in parental education, a proxy measure of developmental exposure to educational resources. Such differences in personal IQ and education are often present among individuals who have illnesses that can strike in adolescence and impair academic achievement. Nonetheless, future work with larger samples should examine the degree to which IQ or education effects may influence outcomes. Additionally, while every effort was made to remove head motion derived artifact, such stringency forced the exclusion of 67 of participants and large number of frames from some of the participants that exceeded the minimum inclusion criteria. The stringent removal of motion artifact by censoring affected frames resulted in slightly different distributions of contiguous frames between the two groups (Fig. S1). This may have differentially affected our ability to fully resolve high-frequency signal components in the data. Future studies will need to address these issues by increasing subject recruitment, aggregating across multiple studies, matching for number of contiguous frames removed, or collecting more data per subject through additional resting state scans or by regressing out of task structure (Cole et al., 2014) to generate pseudo-resting state data. Recruitment of larger studies will have an added benefit of allowing for the investigation of increased variability in connectivity seen across individuals with schizophrenia (reflected in the lower mean within-group NMI in SCZ). This could allow for the study of whether certain aspects of community structure correlate with specific symptom or behavioral dimensions of psychosis (Cuthbert and Insel, 2010). Additionally, the present study examined binarized and thresholded network structures rather than full weighted network structures. While this approach yields analyses that are more computationally tractable than weighted network structures, thresholding the data focuses upon a core set of strongest edges (i.e.: in this study, the edges which were among the strongest 10% to 1% of edges) and may fail to detect effects in edges that are in a lower strength range of the distribution. However, these methods have been informative when applied to the healthy brain (e.g.: (Power et al., 2011)), and thus represent a valid approach to studying how the brain changes with psychopathology. Related to this, the selection of a threshold at which to exclude edges from the graph is a required step and an unsolved issue in the neuroimaging graph theory field. While it is common to examine a range of thresholds, this results in a set of non-independent tie densities, which makes the testing for significance across densities a non-trivial problem.

6. Conclusions

Our findings indicate that while overall network community structure is broadly preserved in adult schizophrenia, there is evidence for statistically significant alterations in the community participation of specific brain regions. These differences were localized to the somatosensory, auditory, default mode, salience, and subcortical networks. These alterations in adult schizophrenia community structure were consistent with alterations observed in childhood-onset schizophrenia, pointing towards some shared etiology between the disorders (Driver et al., 2013; Rapoport and Gogtay, 2011). However, the presence of differences in the findings showing altered connectivity between adult and childhood onset schizophrenia implies that there may be additional and/or different factors involved in the adult form of the disease. Further studies are required to answer these questions and help explain how network structures evolve over time and over the course of this debilitating disease.

Funding

D.B.LS. was supported by the Washington University MSTP Program grant 5T32GM007200; the Cognitive, Computational, and Systems Neuroscience pathway grant 5T32NS073547, and NIH grants 5R01MH066031 and P50MH071616 to D.M.B.. Computations were performed using the facilities of the Washington University Center for High Performance Computing, which were partially provided through grant NCRR 1S10RR022984-01A1.

Conflicts of interest

D.B.LS. reported no conflicts of interest. Dr. Barch consults for Pfizer, Roche, Amgen, and Takeda.

Acknowledgments

We thank: Steve Petersen, Jonathan Power, and Babatunde Adeyemo for creating and sharing MATLAB software tools for resting state fMRI preprocessing and graph theory analyses; Ben Acland and Sachin Dixit for assistance with Freesurfer; and Jo Etzel and Malcolm Tobias for assistance in the use of the Washington University Center for High Performance Computing resources.

Appendix A. Supplementary data

Supplementary data to this article can be found online at http://dx.doi.org/10.1016/j.nicl.2015.11.011.

References

Alexander-Bloch, A.F., Gogtay, N., Meunier, D., Birn, R., Clasen, L., Lalonde, F., Lenroot, R., Giedd, J., Bullmore, E.T., 2010. Disrupted modularity and local connectivity of brain functional networks in childhood-onset schizophrenia. Front. Syst. Neurosci. 4.

Alexander-Bloch, A., Lambiotte, R., Roberts, B., Giedd, J., Gogtay, N., Bullmore, E., 2012. The discovery of population differences in network community structure: new methods and applications to brain functional networks in schizophrenia. NeuroImage 59 (4), 3889–3900.

Anticevic, A., Cole, M.W., Repovs, G., Murray, J.D., Brumbaugh, M.S., Winkler, A.M., Savic, A., Krystal, J.H., Pearlson, G.D., Glahn, D.C., 2014a. Characterizing thalamo-cortical disturbances in schizophrenia and bipolar illness. Cereb. Cortex 24 (12), 3116–3130.

Anticevic, A., Yang, G., Savic, A., Murray, J.D., Cole, M.W., Repovs, G., Pearlson, G.D., Glahn, D.C., 2014b. Mediodorsal and visual thalamic connectivity differ in schizophrenia and bipolar disorder with and without psychosis history. Schizophr. Bull. 40 (6), 1227–1243.

Bassett, D.S., Nelson, B.G., Mueller, B.A., Camchong, J., Lim, K.O., 2012. Altered resting state complexity in schizophrenia. NeuroImage 59 (3), 2196–2207.

Benjamini, Y., Hochberg, Y., 1995. Controlling the false discovery rate: a practical and powerful approach to multiple testing. J. R. Stat. Soc. Ser. B Methodol. 57 (1), 289–300.

Blumensath, T., Jbabdi, S., Glasser, M.F., Van Essen, D.C., Uğurbil, K., Behrens, T.E.J., Smith, S.M., 2013. Spatially constrained hierarchical parcellation of the brain with resting-state fMRI. NeuroImage 76, 313–324.

Bullmore, E., Sporns, O., 2009. Complex brain networks: graph theoretical analysis of structural and functional systems. Nat. Rev. Neurosci. 10 (3), 186–198.

Cole, M.W., Anticevic, A., Repovs, G., Barch, D., 2011. Variable global dysconnectivity and individual differences in schizophrenia. Biol. Psychiatry 70 (1), 43–50.

Cole, M.W., Bassett, D.S., Power, J.D., Braver, T.S., Petersen, S.E., 2014. Intrinsic and task-evoked network architectures of the human brain. Neuron 83 (1), 238–251.

Cuthbert, B.N., Insel, T.R., 2010. Toward new approaches to psychotic disorders: the NIMH research domain criteria project. Schizophr. Bull. 36 (6), 1061–1062.

Cuthbert, B.N., Kozak, M.J., 2013. Constructing constructs for psychopathology: the NIMH research domain criteria. J. Abnorm. Psychol. 122 (3), 928–937.

Dosenbach, N.U.F., Fair, D.A., Miezin, F.M., Cohen, A.L., Wenger, K.K., Dosenbach, R.A.T., Fox, M.D., Snyder, A.Z., Vincent, J.L., Raichle, M.E., Schlaggar, B.L., Petersen, S.E., 2007. Distinct brain networks for adaptive and stable task control in humans. Proc. Natl. Acad. Sci. U. S. A. 104 (26), 11073–11078.

Driver, D.I., Gogtay, N., Rapoport, J.L., 2013. Childhood onset schizophrenia and early onset schizophrenia spectrum disorders. Child Adolesc. Psychiatr. Clin. N. Am. 22 (4), 539–555.

Ellison-Wright, I., Bullmore, E., 2009. Meta-analysis of diffusion tensor imaging studies in schizophrenia. Schizophr. Res. 108 (1–3), 3–10.
Fornito, A., Zalesky, A., Pantelis, C., Bullmore, E.T., 2012. Schizophrenia, neuroimaging and connectomics. NeuroImage 1–19.
Fortunato, S., 2010. Community detection in graphs. Phys. Rep. 486 (3–5), 75–174.
Fox, M.D., Snyder, A.Z., Vincent, J.L., Corbetta, M., Van Essen, D.C., Raichle, M.E., 2005. The human brain is intrinsically organized into dynamic, anticorrelated functional networks. Proc. Natl. Acad. Sci. 102 (27), 9673–9678.
Friston, K.J., Williams, S., Howard, R., Frackowiak, R.S., Turner, R., 1996. Movement-related effects in fMRI time-series. Magn. Reson. Med. 35, 346–355.
Friston, K.J., 1998. The disconnection hypothesis. Schizophr. Res. 30 (2), 115–125.
Glahn, D.C., Winkler, A.M., Kochunov, P., Almasy, L., Duggirala, R., Carless, M.A., Curran, J.C., Olvera, R.L., Laird, A.R., Smith, S.M., Beckmann, C.F., Fox, P.T., Blangero, J., 2010. Genetic control over the resting brain. Proc. Natl. Acad. Sci. 107 (3), 1223–1228.
Jafri, M.J., Pearlson, G.D., Stevens, M., Calhoun, V.D., 2008. A method for functional network connectivity among spatially independent resting-state components in schizophrenia. NeuroImage 39 (4), 1666–1681.
Jiang, T., Zhou, Y., Liu, B., Liu, Y., Song, M., 2013. Brainnetome-wide association studies in schizophrenia: the advances and future. Neurosci. Biobehav. Rev. 37 (10), 2818–2835.
Liu, Y., Liang, M., Zhou, Y., He, Y., Hao, Y., Song, M., Yu, C., Liu, H., Liu, Z., Jiang, T., 2008. Disrupted small-world networks in schizophrenia. Brain 131 (4), 945–961.
Lynall, M.E., Bassett, D.S., Kerwin, R., McKenna, P.J., Kitzbichler, M., Muller, U., Bullmore, E., 2010. Functional connectivity and brain networks in schizophrenia. J. Neurosci. 30 (28), 9477–9487.
Ma, S., Calhoun, V.D., Eichele, T., Du, W., Adalı, T., 2012. Modulations of functional connectivity in the healthy and schizophrenia groups during task and rest. NeuroImage 62 (3), 1694–1704.
Manning, C.D., Raghavan, P., Schutze, H., 2008. Introduction to Information Retrieval. Cambridge University Press.
Moran, L.V., Tagamets, M.A., Sampath, H., O'Donnell, A., Stein, E.A., Kochunov, P., Hong, L.E., 2013. Disruption of anterior insula modulation of large-scale brain networks in schizophrenia. Biol. Psychiatry 74 (6), 467–474.
Newman, M.E.J., 2006. Modularity and community structure in networks. Proc. Natl. Acad. Sci. 103 (23), 8577–8582.
Öngür, D., Lundy, M., Greenhouse, I., Shinn, A.K., Menon, V., Cohen, B.M., Renshaw, P.F., 2010. Default mode network abnormalities in bipolar disorder and schizophrenia. Psychiatry Res. 183 (1), 59–68.
Palaniyappan, L., Simmonite, M., White, T.P., Liddle, E.B., Liddle, P.F., 2013. Neural primacy of the salience processing system in schizophrenia. Neuron 79 (4), 814–828.
Patel, S., Mahon, K., Wellington, R., Zhang, J., Chaplin, W., Szeszko, P.R., 2011. A meta-analysis of diffusion tensor imaging studies of the corpus callosum in schizophrenia. Schizophr. Res. 129 (2–3), 149–155.
Pettersson-Yeo, W., Allen, P., Benetti, S., McGuire, P., Mechelli, A., 2011. Dysconnectivity in schizophrenia: where are we now? Neurosci. Biobehav. Rev. 35 (5), 1110–1124.
Power, J.D., Cohen, A.L., Nelson, S.M., Wig, G.S., Barnes, K.A., Church, J.A., Vogel, A.C., Laumann, T.O., Miezin, F.M., Schlaggar, B.L., Petersen, S.E., 2011. Functional network organization of the human brain. Neuron 72 (4), 665–678.
Power, J.D., Barnes, K.A., Snyder, A.Z., Schlaggar, B.L., Petersen, S.E., 2012. Spurious but systematic correlations in functional connectivity MRI networks arise from subject motion. NeuroImage 59 (3), 2142–2154.
Power, J.D., Mitra, A., Laumann, T.O., Snyder, A.Z., Schlaggar, B.L., Petersen, S.E., 2014. Methods to detect, characterize, and remove motion artifact in resting state fMRI. NeuroImage 84, 320–341.
Rapoport, J.L., Gogtay, N., 2011. Childhood onset schizophrenia: support for a progressive neurodevelopmental disorder. Int. J. Dev. Neurosci. 29 (3), 251–258.
Repovs, G., Csernansky, J.G., Barch, D.M., 2011. Brain network connectivity in individuals with schizophrenia and their siblings. Biol. Psychiatry 69 (10), 967–973.
Rosvall, M., Bergstrom, C.T., 2008. Maps of random walks on complex networks reveal community structure. Proc. Natl. Acad. Sci. 105 (4), 1118–1123.
Rubinov, M., Bullmore, E., 2013. Schizophrenia and abnormal brain network hubs. Dialogues Clin. Neurosci. 15 (3), 339–349.
Rubinov, M., Sporns, O., 2010. Complex network measures of brain connectivity: uses and interpretations. NeuroImage 52 (3), 1059–1069.
Satterthwaite, T.D., Wolf, D.H., Loughead, J., Ruparel, K., Elliott, M.A., Hakonarson, H., Gur, R.C., Gur, R.E., 2012. Impact of in-scanner head motion on multiple measures of functional connectivity: relevance for studies of neurodevelopment in youth. NeuroImage 60 (1), 623–632.
Sheffield, J.M., Repovs, G., Harms, M.P., Carter, C.S., Gold, J.M., MacDonald III, A.W., Daniel Ragland, J., Silverstein, S.M., Godwin, D., Barch, D.M., 2015. Fronto-parietal and cingulo-opercular network integrity and cognition in health and schizophrenia. Neuropsychologia 73, 82–93.
Stephan, K.E., Baldeweg, T., Friston, K.J., 2006. Synaptic plasticity and dysconnection in schizophrenia. BPS 59 (10), 929–939.
van den Heuvel, M.P., Fornito, A., 2014. Brain networks in schizophrenia. Neuropsychol. Rev. 24 (1), 32–48.
Van Dijk, K.R.A., Sabuncu, M.R., Buckner, R.L., 2012. The influence of head motion on intrinsic functional connectivity MRI. NeuroImage 59 (1), 431–438.
Van Essen, D.C., 2005. A population-average, landmark- and surface-based (PALS) atlas of human cerebral cortex. NeuroImage 28 (3), 635–662.
Van Essen, D.C., Dierker, D.L., 2007. Surface-based and probabilistic atlases of primate cerebral cortex. Neuron 56 (2), 209–225.
Van Essen, D.C., Drury, H.A., Dickson, J., Harwell, J., Hanlon, D., Anderson, C.H., 2001. An integrated software suite for surface-based analyses of cerebral cortex. J. Am. Med. Inform. Assoc. 8 (5), 443–459.
Whitfield-Gabrieli, S., Thermenos, H.W., Milanovic, S., Tsuang, M.T., Faraone, S.V., McCarley, R.W., Shenton, M.E., Green, A.I., Nieto-Castanon, A., LaViolette, P., Wojcik, J., Gabrieli, J.D.E., Seidman, L.J., 2009. Hyperactivity and hyperconnectivity of the default network in schizophrenia and in first-degree relatives of persons with schizophrenia. Proc. Natl. Acad. Sci. U. S. A. 106 (4), 1279–1284.
Woodward, N.D., Heckers, S., 2015. Mapping thalamocortical functional connectivity in chronic and early stages of psychotic disorders. Biol. Psychiatry http://dx.doi.org/10.1016/j.biopsych.2015.06.026 (in press).
Woodward, N.D., Rogers, B., Heckers, S., 2011. Functional resting-state networks are differentially affected in schizophrenia. Schizophr. Res. 130 (1–3), 86–93.
Woodward, N.D., Karbasforoushan, H., Heckers, S., 2012. Thalamocortical dysconnectivity in schizophrenia. Am. J. Psychiatry 169 (10), 1092–1099.
Zhou, Y., Liang, M., Jiang, T., Tian, L., Liu, Y., Liu, Z., Liu, H., Kuang, F., 2007. Functional dysconnectivity of the dorsolateral prefrontal cortex in first-episode schizophrenia using resting-state fMRI. Neurosci. Lett. 417 (3), 297–302.